Available online at www.sciencedirect.com
SCIENCE DIRECT®
Journal of Petroleum Science and Engineering 51 (2006) 68–84
JOURNAL OF PETROLEUM SCIENCE & ENGINEERING
www.elsevier.com/locate/petrol

Correction of basic equations for deep bed filtration with dispersion

J.E. Altoé F. [a], P. Bedrikovetsky [a,*], A.G. Siqueira [b], A.L.S. de Souza [b], F.S. Shecaira [b]

[a] *Department of Petroleum Exploration and Production Engineering, North Fluminense State University Lenep/UENF, Rod. Amaral Peixoto, km 163 – Av. Brenand, s/n° Imboacica – Macaé, RJ 27.925-310, Brazil*
[b] *Petrobras/Cenpes, Cidade Universitaria Q.7, Ilha Do Fundão, 21949-900 – Rio De Janeiro — RJ, Brazil*

Accepted 4 November 2005

Abstract

Deep bed filtration of particle suspensions in porous media occurs during water injection into oil reservoirs, drilling fluid invasion into reservoir productive zones, fines migration in oil fields, bacteria, virus or contaminant transport in groundwater, industrial filtering, etc. The basic features of the process are advective and dispersive particle transport and particle capture by the porous medium.

Particle transport in porous media is determined by advective flow of carrier water and by hydrodynamic dispersion in micro-heterogeneous media. Thus, the particle flux is the sum of advective and dispersive fluxes. Transport of particles in porous media is described by an advection–diffusion equation and by a kinetic equation of particle capture. Conventional models for deep bed filtration take into account hydrodynamic particle dispersion in the mass balance equation but do not consider the effect of dispersive flux on retention kinetics.

In the present study, a model for deep bed filtration with particle size exclusion taking into account particle hydrodynamic dispersion in both mass balance and retention kinetics equations is proposed. Analytical solutions are obtained for flows in infinite and semi-infinite reservoirs and in finite porous columns. The physical interpretation of the steady-state flow regimes described by the proposed and the traditional models favours the former.

Comparative matching of experimental data on particle transport in porous columns by the two models is performed for two sets of laboratory data.

Keywords: Deep bed filtration; Dispersion; Suspension; Governing equations; Modelling; Porous media; Emulsion

1. Introduction

Severe injectivity decline during sea/produced water injection is a serious problem in offshore waterflood projects. The permeability impairment occurs due to capture of particles from injected water by the rock. The reliable modelling-based prediction of injectivity decline is important for the injected-water-treatment design, for injected water management (injection of sea- or produced water, their combinations, water filtering), etc.

The formation damage induced by penetration of drilling fluid into a reservoir also occurs due to particle capture by rocks and consequent permeability reduction. Other petroleum applications include sand production control, fines migration and deep bed filtration in gravel packs.

* Corresponding author. Tel.: +55 22 27733391; fax: +55 22 27969734.
E-mail addresses: pavel@lenep.uenf.br, pavel.russia@gmail.com (P. Bedrikovetsky).

0920-4105/$ - see front matter © 2006 Elsevier B.V. All rights reserved.
doi:10.1016/j.petrol.2005.11.010

The basic equations for deep bed filtration taking into account advective particle transport and the kinetics of particle retention, and neglecting hydrodynamic dispersion have been derived essentially following the filtration equation proposed by Iwasaki (1937). A number of predictive models have been presented in the literature (Sharma and Yortsos, 1987a,b,c; Elimelech et al., 1995; Tiab and Donaldson, 1996, Khilar and Fogler, 1998; Logan, 2001). The equations allow for various analytical solutions, which have been used for the treatment of laboratory data and for prediction of porous media contamination and clogging (Herzig et al., 1970; Pang and Sharma, 1994; Wennberg and Sharma, 1997; Harter et al., 2000; Bedrikovetsky et al., 2001, 2002).

However, particle dispersion in heterogeneous porous media is important for both small and large scales (Lake, 1989; Jensen et al., 1997). The typical core sizes in laboratory experiments are small, and hence the Peclet number is relatively high. The typical dispersivity values for large formation scales are high, and consequently the Peclet number may also take high values. The Peclet number for either situation may amount up to 10–20.

The effect of dispersion on deep bed filtration is particularly important near to wells, where the dispersivity may already arise to the bed scale, and the formation damage occurs in one two-meter neighbourhood.

Therefore, several deep bed filtration studies take into account dispersion of particles (Grolimund et al., 1998; Kretzschmar et al., 1997; Bolster et al., 1998; Unice and Logan, 2000; Logan, 2001; Tufenkji et al., 2003). A detailed description of such early work is presented in the review paper by Herzig et al. (1970). The models developed account for particle dispersion in the mass balance for particles but do not consider the dispersion flux contribution to the retention kinetics.

In the present study, the proposed deep bed filtration model takes into account dispersion in both the equation of mass balance and in that of capture kinetics. Several analytical models for constant filtration coefficient and for dynamic blocking filtration coefficient have been developed. If compared with the traditional model, the proposed model exhibits more realistic physics behaviour. The difference between the traditional and proposed model is significant for small Peclet numbers.

The structure of the paper is as follows. In Section 2 we formulate the corrected model for deep bed filtration of particulate suspensions in porous media accounting for hydrodynamic dispersion of suspended particles. The dispersion-free deep bed filtration model is presented in Section 3 as a particulate case of the general system with dispersion. The analytical models for flow in infinite and semi-infinite reservoirs for constant filtration coefficient are presented in Sections 4 and 5, respectively. An analytical solution for deep bed filtration in semi-infinite reservoirs with the fixed inlet concentration is given in Section 6. Analytical steady state solution for laboratory coreflood in discussed in Section 7. The analytical models allow for laboratory data treatment (Section 8). Travelling wave flow regimes for dynamic blocking filtration coefficient are described in Section 9. In Section 10, three dimensional equations for deep bed filtration with dispersion are derived. Mathematical details of the derivations are presented in Appendices. Dimensionless form of governing equations and initial-boundary conditions are given in Appendix A. The transient solutions for flow in infinite and semi-infinite reservoirs and constant filtration coefficient are derived in Appendices B, C and D. Appendix E contains derivations for steady state solution in a finite core. Appendix F contains derivations for travelling wave flow.

2. Model formulation

Let us derive governing equations for deep bed filtration taking into account particle dispersion. The usual assumptions of constant suspension density and porosity for low particle concentrations are adopted. The balance equation for suspended and retained particles (Iwasaki, 1937; Herzig et al., 1970) is:

$$\frac{\partial}{\partial t}(\phi c + \sigma) + \frac{\partial q}{\partial x} = 0 \tag{1}$$

Here, the concentration c is a number of suspended particles per unit volume of the fluid, and the retained particle concentration σ is a number of captured particles per unit volume of the rock.

The particle flux q consists of the advective and dispersive components:

$$q = Uc - D\frac{\partial c}{\partial x} \tag{2}$$

$$D = \alpha_D U \tag{3}$$

Here the dispersion coefficient D is assumed to be proportional to the flow velocity U, and the proportionality coefficient α_D is called the longitudinal dispersivity (Lake, 1989; Nikolaevskij, 1990; Sorbie, 1991).

Let us consider the following physical model for the size exclusion particle capture in porous media (Santos and Bedrikovetsky, 2005). Particles are not captured during flow through the pore system, but there is a

sequence of particle capturing sieves perpendicular to the flow direction. The probability for a particle to be captured is equal to λl (l is the distance between the sieves), and that to pass through is $1-\lambda l$. In other words, after particles pass the distance l, their flux reduces $1-\lambda l$ times.

So, the so called filtration coefficient λ is determined through the fraction λl of the particle flux that remains in porous media during flow along the distance l (Iwasaki, 1937). The filtration coefficient λ is the probability for particle to be captured during the flow over the unit distance; its dimension is L^{-1}.

Following the probabilistic interpretation of filtration coefficient, Herzig et al. (1970) have calculated the number of captured particles per unit time per unit volume during advective flow. Let us calculate the deposition rate for advective–dispersive flow. The number of particles crossing sieve during time Δt is equal to $qA\Delta t$, where A is a cross section area. The particles move along the distance $U\Delta t/\varphi$ during this time, here φ is the porosity. The probability for particle to be captured is $\lambda U\Delta t/\varphi$. Particle retention takes place in the volume $AU\Delta t/\varphi$. The deposition rate is

$$\frac{\Delta\sigma}{\Delta t}=\frac{(qA\Delta t)(\lambda U\Delta t/\phi)}{(AU\Delta t/\phi)\Delta t}=\lambda q$$

So, the interpretation of the capture rate in terms of probability for the particle capture in elementary reference volume implies that the capture rate is proportional to the total particle flux (Eq. (2)) rather than just to its advective component.

From now on we assume that the particle capture rate is proportional to the overall particle flux (first-order particle retention kinetics):

$$\frac{\partial\sigma}{\partial t}=\lambda(\sigma)q \tag{4}$$

Here the filtration coefficient $\lambda(\sigma)$ is a function of retained concentration σ. Particle deposition changes the pore space geometry and, consequently, the conditions for size exclusion capture, so the deposition rate should be retained-concentration-dependent.

Fig. 1 illustrates size exclusion capture of particles — a pore captures a particle if the particle size exceeds the pore size, otherwise the particle passes through the pore. Therefore, the capture rate must be proportional to the total particle flux. A particle is captured by a pore regardless of whether the advective or dispersive flux has brought the particle to the pore.

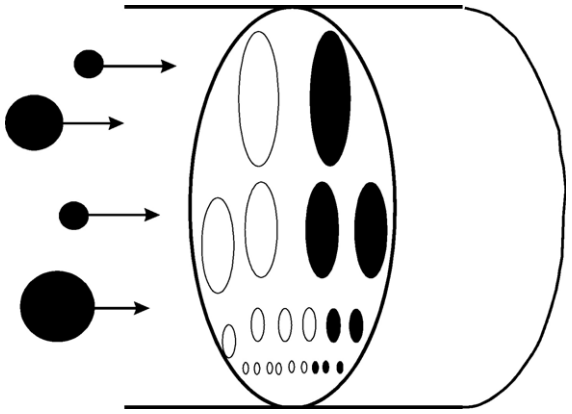

Fig. 1. Schema for particle capture by size exclusion in deep bed filtration.

The same applies to bridging build-up and to the consequent particle capture (Payatakes et al., 1974; Elimelech et al., 1995).

It is worth mentioning that usually size exclusion is not dominant in virus and bacteria capture during their flow in porous media. The retention mainly happens due to sorption (Kuhnen et al., 2000). In this case, the authors assume that the deposition rate is proportional to suspended concentration only. The proportionality coefficient dimension is $1/T$, i.e. the proportionality coefficient is a probability for particle to be captured during the unitary time. In this case, neither hydrodynamic dispersion nor advective velocity enters in the capture rate expression.

The same applies to chemical reactions and dissolution in porous media (Kechagia et al., 2002).

Many experiments show that during the particle suspension flow in porous media, the particle capture rate rapidly decreases as particles start to accumulate on the collectors; the retention stops when the retained concentration reaches some critical value (Elimelech et al., 1995; Kuhnen et al., 2000). This phenomenon is called blocking. It can be explained by decrease of the number of vacancies for further retention during the retention process.

For example, if the injected particle sizes are comparable with pore throats sizes, the particles are captured by pore size exclusion. Consider a wide throat size distribution, and injection of particles with intermediate sizes. Particles are captured in smaller pores. When all small pores are filled, the suspension flows through thick throats, and the particles are not captured any more.

Hereafter the following features of the filtration blocking coefficient $\lambda(\sigma)$ are assumed:

$$0<\sigma<\sigma_m:\lambda(\sigma)>0;\sigma\geq\sigma_m:\lambda(\sigma)=0 \tag{5}$$

The important particular case of Eq. (5) is the linear filtration coefficient

$$\lambda(\sigma) = \lambda_0(1 - b\sigma) \tag{6}$$

so called Langmuir blocking function (Kuhnen et al., 2000). It is typical where the capture is realized by a mono-layer adsorption.

This case corresponds to the situation where one vacancy can be filled by one particle. So, retention of some particles results in filling of the same number of vacancies, i.e. the total of deposited particle concentration $\sigma(x,t)$ and the vacant pore concentration $h(x,t)$ is equal to initial concentration of vacancies $h(x,0)$:

$$h(x,t) = h(x,0) - \sigma(x,t) \tag{7}$$

The capture rate is proportional to the product of particle flux and vacancy concentration (acting mass law). Using Eq. (7), we obtain:

$$\frac{\partial \sigma}{\partial t} = \lambda_0\left(1 - \frac{\sigma}{h(x,0)}\right)q \tag{8}$$

The filtration function $\lambda(\sigma)$ depends on porous media structure. Therefore, for heterogeneous porous media where initial vacancy concentration depends on x, the filtration function is x-dependent: $\lambda = \lambda(\sigma, x)$. Further in the paper we assume a uniform initial vacancy concentration and use the dependency $\lambda = \lambda(\sigma)$.

So, the Langmuir linear blocking function (Eq. (6)) corresponds to "one particle – one pore" kinetics [Eq. (8)]. The comparison of formulae Eqs. (8) and (4) results in Eq. (6).

If λ_0 in Eq. (8) is also a function of σ, the blocking filtration coefficient $\lambda(\sigma)$ is non-linear.

Darcy's law for suspension flow in porous media includes the effect of permeability decline during particle retention:

$$U = -\frac{k_0 k(\sigma)}{\mu}\frac{\partial p}{\partial x} \tag{9}$$

$$k(\sigma) = \frac{1}{1 + \beta\sigma} \tag{10}$$

Here $k(\sigma)$ is called the permeability reduction function, and β is the formation damage coefficient.

Eqs. (1), (2), (4) and (9) form a closed system of four equations that govern the colloid filtration with size exclusion particle capture in porous media. The unknowns are suspended concentration c, deposited σ, particle flux q and pressure p.

The independence of the filtration and dispersion coefficients of pressure allows separation of Eqs. (1), (2) and (4) from Eq. (9), which means that the suspended and retained concentrations and the particle flux can be found from the system of Eqs. (1), (2) and (4) and then the pressure distribution can be found from Eq. (9).

Form of the system of governing equations in non-dimensional co-ordinates is presented in Appendix A, (Eqs. (A-2)–(A-5)). The system contains the dimensionless parameter ε_D that is the inverse to the Peclet number; it is equal to the dispersion-to-advective flux ratio (Nikolaevskij, 1990). From Eq. (3) it follows that:

$$\varepsilon_D = \frac{1}{\mathrm{Pe}} = \frac{D}{LU} = \frac{\alpha_D}{L} \tag{11}$$

The dispersion–advective ratio ε_D is equal to the ratio between the micro heterogeneity size α_D (dispersivity) and the reference size of the boundary problem L.

Let us estimate the contribution of dispersion to the total particle flux (Eq. (2)). In the majority of papers, deep bed filtration model has been modelled under the laboratory floods conditions, where homogeneous sand columns are employed (Elimelech et al., 1995; Unice and Logan, 2000; Tufenkji et al., 2003). On the core scale in homogeneous cores, we have L~0.1 m, α_D~0.001 m, ε_D~0.01, and hence the dispersion can be neglected. In natural heterogeneous cores, ε_D can amount to 0.1 or more, and dispersion should be taken into account (Lake, 1989; Bedrikovetsky, 1993). In a well neighbourhood, the reference radius of formation damage zone is 1 m, the heterogeneity reference size is also 1 m, so ε_D has order of magnitude of unity.

The dispersivity α_D can reach several tens or even hundreds of meters at formation scales (Lake, 1989; Jensen et al., 1997); thus, the dimensionless dispersion can have the order of magnitude of unity, and hence hydrodynamic dispersion should be taken into account.

Now we formulate one dimensional problem for suspension injection into a porous core/reservoir.

The absence of suspended and retained particles in porous media before the injection is represented by the initial conditions:

$$t = 0 : c = \sigma = 0 \tag{12}$$

Fixing the inlet particle flux during the injection of particulate suspension in a reservoir determines the boundary condition:

$$x = 0 : Uc - D\frac{\partial c}{\partial x} = c^0 U \tag{13}$$

Sometimes the dispersive term in the boundary condition (Eq. (13)) is neglected (van Genuchten, 1981 and Nikolaevskij, 1990):

$$x = 0 : c = c^0 \tag{14}$$

The particle motion in porous media can be decomposed into an advective flow with constant velocity and the dispersive random walks around the front that moves with advective velocity (Kampen, 1984). It is assumed that once a particle leaves the core outlet by advection it cannot come back by dispersion. This assumption leads to the boundary condition of absence of dispersion at the core outlet (Danckwerts, 1953; Nikolaevskij, 1990):

$$x = L : \frac{\partial c}{\partial x} = 0 \tag{15}$$

In dimensionless coordinates (Eq. (A-1)), the proposed model with a constant filtration coefficient takes the form (Eqs. (A-10) and (11)):

$$\frac{\partial C}{\partial T} + v\frac{\partial C}{\partial X} = \varepsilon_D \frac{\partial^2 C}{\partial X^2} - \Lambda C \tag{16}$$

$$v = 1 - \Lambda\varepsilon_D \tag{17}$$

Neglecting the dispersion term in the capture kinetics Eqs. (16) and (17) results in:

$$\frac{\partial C}{\partial T} + \frac{\partial C}{\partial X} = \varepsilon_D \frac{\partial^2 C}{\partial X^2} - \Lambda C \tag{18}$$

Eq. (18) is a traditional advective–diffusive model with a sink term. The boundary condition (Eq. (13)) fixes the inlet flux in this model.

Eq. (16) looks like the advective–diffusive model (Eq. (18)) with advective velocity v, and seems this velocity should appear in the expression for the inlet flux (Eq. (13)). However, the real advective velocity in Eq. (16) is equal to one, and the delay term $-\Lambda\varepsilon_D$ appears due to the capture of particles transported by the dispersive flux and is not a part of the flux. From conservation law (Eqs. (1) and (A-2)) it follows that the particle flux is continuous at the inlet; the boundary condition for Eq. (16) should be given by Eq. (13) that differs from the inlet boundary condition for the equivalent advective–diffusive model with the advective velocity v.

Following Logan (2001), from now on the model (Eq. (18)) will be referred to as the HLL model in order to honour the fundamental work by Herzig et al. (1970).

The difference between the presented and the HLL model is the delay term $\Lambda\varepsilon_D$ that appears in the advective flux velocity (Eq. (17)). This is the collective effect of the particle dispersion and capture. Appearance of the delay term $\Lambda\varepsilon_D$ in the advective flux velocity (Eq. (17)) is due to accounting for diffusive flux in the capture kinetics (Eq. (2) and Eq. (4)).

A delay in the particle pulse arrival to the column effluent if compared with the tracer pulse breakthrough was observed by Massei et al. (2002).

The length L used in dimensionless parameters (Eq. (A-1)) is a reference size of the boundary problem. It affects the dimensionless filtration coefficient Λ (Eq. (A-1)) and the inverse to Peclet number ε_D, (Eq. (11)) and drops out the delay term: $\Lambda\varepsilon_D = \lambda\alpha_D$. The dimensionless time T corresponding to the length L (Eq. (A-1)) is measured in "pore volume injected", which is the common unit in laboratory coreflooding and in field data presentation.

Also, often the injected suspension is traced, and the particle breakthrough curves are presented together with tracer curves (Jin et al., 1997; Ginn, 2000). In this case, the inverse to Peclet number ε_D in Eq. (16) is already known from the tracer data and it is convenient to use dimensionless variables and parameters (Eq. (A-1)).

Nevertheless, Eq. (16) depends on two independent dimensionless parameters —ε_D and Λ.

The inverse to filtration coefficient is an average penetration depth of suspended particles (Herzig et al., 1970), so the inverse to reference value of filtration coefficient $1/\lambda_0$ can be used as a reference length in dimensionless linear co-ordinate (Eq. (A-12)). For corresponding dimensionless variables (Eq. (A-12)), the dimensionless Λ becomes equal to unit in the case of constant filtration coefficient, and Eq. (16) becomes dependent of one dimensionless parameter ε only, (Eq. (A-13)):

$$\frac{\partial C}{\partial T'} + v\frac{\partial C}{\partial X'} = \varepsilon \frac{\partial^2 C}{\partial X'^2} - C \tag{19}$$

$$v = 1 - \varepsilon,\ \ \varepsilon = \lambda_0\alpha_D$$

In the case of filtration function $\Lambda = \Lambda(S)$, Eq. (16) includes deposited concentration S, and the model consists of two equations

$$\begin{aligned} &\frac{\partial C}{\partial T} + (1 - \Lambda(S)\varepsilon_D)\frac{\partial C}{\partial X} = \varepsilon_D \frac{\partial^2 C}{\partial X^2} - \Lambda(S)C \\ &\frac{\partial S}{\partial T} = \Lambda(S)\left(1 - \varepsilon_D \frac{\partial C}{\partial X}\right) \end{aligned} \tag{20}$$

for dimensionless parameters (Eq. (A-1)).

For dimensionless variables (Eq. (A-12)), ε_D must be changed to $\varepsilon = \lambda_0\alpha_D$.

The HLL in this case is also obtained by neglecting dispersion term in capture rate expression.

The order of the governing system (Eq. (20)) can be reduced by one. Introducing the function

$$\Phi(S) = \int_0^S \frac{1}{\Lambda(s)} ds \tag{21}$$

from Eq. (A-3) we obtain:

$$\frac{\partial \Phi(S)}{\partial T} = Q \tag{22}$$

Substitution of Eq. (22) into Eq. (A-2) results in

$$\frac{\partial}{\partial T}(C+S) + \frac{\partial}{\partial X}\left(\frac{\partial \Phi(S)}{\partial T}\right) = 0 \tag{23}$$

Changing order of differentiation in the second term in the right hand side of Eq. (23) and integrating in T from zero to T, we obtain first order partial differential equation:

$$C + S + \frac{\partial \Phi(S)}{\partial X} = 0 \tag{24}$$

The integration constant that should appear in right hand side of Eq. (24) was calculated from initial conditions (Eq. (12)) — it is equal zero.

Eq. (22) becomes

$$\frac{\partial \Phi(S)}{\partial T} = 1 - \varepsilon_D \frac{\partial C}{\partial X} \tag{25}$$

Eqs. (24) and (25) form quasi-linear system of first order equations modeling deep bed filtration with size exclusion particle capture accounting for dispersion.

3. Dispersion free model

Neglecting the dispersion in Eq. (16) results in the simplified deep bed filtration model (Sharma and Yortsos, 1987a,b,c; Elimelech et al., 1995; Tiab and Donaldson, 1996):

$$\frac{\partial C}{\partial T} + \frac{\partial C}{\partial X} = -\Lambda C \tag{26}$$

The boundary condition (Eq. (13)) automatically takes the form of Eq. (14).

The solution of the dispersion-free deep bed filtration problem (Eqs. (26) (12) and (14)) is given by

$$C(X,T) = \begin{cases} \exp(-\Lambda X) & X \le T \\ 0 & X > T \end{cases} \tag{27}$$

Concentration is zero ahead of the concentration front $X_0(T)=T$. Particles arrive at the column outlet after one pore volume injection. Once the advancing front passes a given location, a steady concentration distribution is immediately established behind the front.

4. Transient flow in infinite reservoir

Let us consider flow in an infinite reservoir where, initially, water with particles fills the semi-infinite reservoir $X<0$, and clean water fills the semi-infinite reservoir $X>0$. Formula for concentration wave propagation (Eq. (B-2)) is presented in Appendix B.

Fig. 2 shows the concentration profiles for the times $T=0.1$, 1.0 and 4.0 with $\varepsilon_D=1.0$ and $\Lambda=0.5$. Solid lines correspond to the proposed model and dotted lines correspond to the HLL model. Both models exhibit advective propagation of the concentration wave with diffusive smoothing of the initial shock; the mixture zone expands with time. Suspended concentration is zero ahead of the mixture zone. Behind the mixture zone, concentration does not vary along the reservoir and exponentially decays with time due to deep bed filtration with a constant filtration coefficient. One can observe a delay in the concentration front propagation for the proposed model (Eq. (16)) if compared with the HLL model (Eq. (18)). The difference in the profiles in the two models appears in the mixture zone, while the concentrations ahead of and behind the mixture zone coincide for both models.

5. Analytical model for suspension injection into semi-infinite reservoir

In this section we consider the particulate suspension injection into a semi-infinite reservoir, $X>0$. The expression for suspension concentration (Eq. (C-2)) is presented in Appendix C.

Fig. 3 epicts particle flux profiles for the dispersi shows the concentration profiles at the moments $T=0.5$, 1.0, 2.0 and 6.0 as obtained by explicit formula

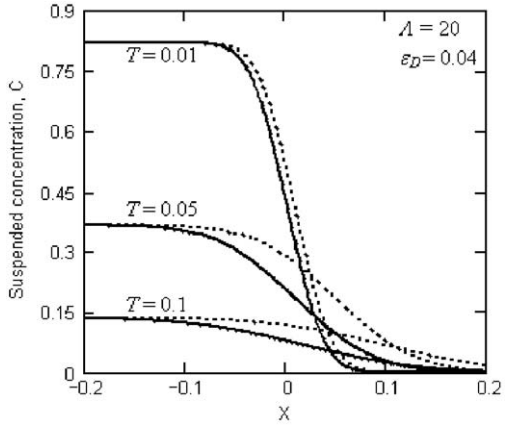

Fig. 2. Concentration wave dynamics in an infinite reservoir by the presented model and by the HLL model.

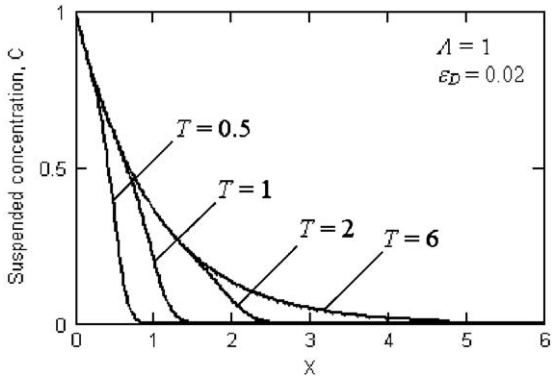

Fig. 3. Dynamics of concentration waves in a semi-infinite reservoir.

(Eq. (C-2)). The envelope curve corresponds to steady-state solution (Eq. (C-5)). Furthermore, for any moment T there exists such position of a mixture zone $X_0(T)$ that the transient and steady-state profiles behind the zone ($X<X_0(T)$) almost coincide. Once the transition zone passes a given location, the steady-state suspended concentration distribution is established behind. After establishing the steady state, all newly arrived particles are captured by the rock, and the suspended concentration is time-independent.

The term "steady state" is applied to the suspended concentration only. The retained concentration increases during the flow.

The particle flux profile in the steady-state regime (Eq. (C-6)) shows that the λth fraction of the particle flux is captured under the steady-state conditions, and $(1-\lambda)$th fraction passes through. The result must be independent of the particle flux partition into the advective and dispersive parts, i.e. the formula for the steady-state flux profile must not contain the dispersion coefficient (Eq. (C-6)).

Fig. 4 depicts particle flux profiles for the dispersion-free model (solid line) and for the proposed model using the solution (Eq. (C-5)) (dotted line) for $\varepsilon_D=0.002$ and $\Lambda=1$. The suspended concentration and the particle flux coincide for dispersion-free flow, and the profile is discontinuous. The introduction of particle dispersion leads to smoothing of the shock. The larger is the dispersion coefficient, the wider is the smoothed zone around the shock.

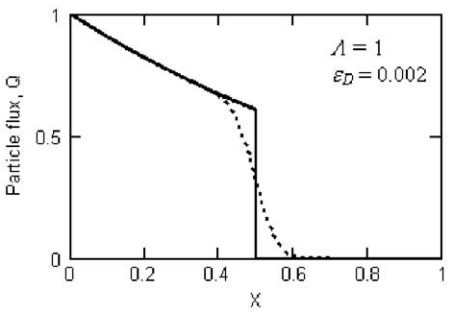

Fig. 4. Particle flux profile for $T=0.5$ (semi-infinite reservoir) by the proposed model and the dispersion-free model.

Fig. 5 presents particle flux histories at the point $X=1$ in a semi-infinite reservoir for the dispersion-free case (curve $\varepsilon_D=0$) and three different dispersion values $\varepsilon_D=0.01$, 0.1 and 0.5. On the one side, the higher is the dispersion, the larger is the delay in the arrival of the concentration front. On the other side, the larger is the dispersion, the wider is the mixture zone about the shock. Thus, the effect of the delay in advection competes with that of the dispersion zone expansion. Fig. 5 shows fast breakthrough for large dispersion values.

Let us compare the stationary particle flux profiles behind the moving mixture zone as obtained by the proposed and HLL models. The solution can be obtained from Eq. (C-2) by setting $v=1$ and tending T to infinity. The calculation of the flux profile shows that it is dispersion-dependent.

The asymptotic steady-state particle flux profile (Eq. (C-6)) for the presented model coincides with that for the dispersion-free model and is dispersion-independent.

The comparative results are displayed in Fig. 6. The flux is equal to 0.37 at $X=1$ for both the proposed and dispersion-free models. The HLL model profiles were calculated for $\varepsilon_D=0.1$, 1.0 and 3.0; the corresponding particle fluxes at $X=1$ were found to be 0.40, 0.54 and 0.65, respectively.

The directions of diffusive and advective fluxes coincide. Therefore, inclusion of the diffusive flux into the particle capture rate (Eq. (4)) increases the retention, and the flux profile as calculated by the proposed model is located below that as obtained by HLL model (Fig. 6).

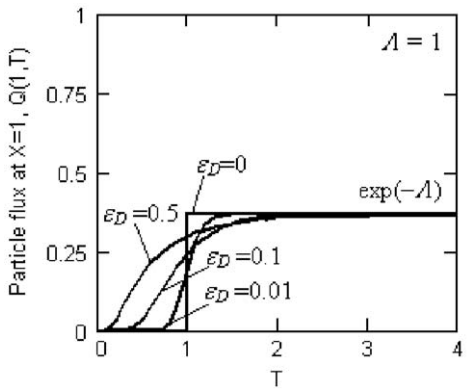

Fig. 5. Particle flux history at the point $X=1$ in semi-infinite reservoir for different dispersion coefficients.

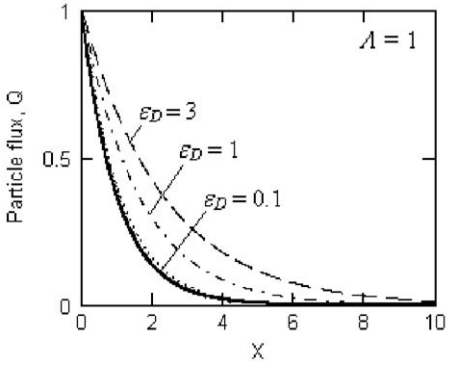

Fig. 6. Steady-state particle flux profiles for the dispersion-free case and by the presented model (the same solid curve) and by the HLL model with ε_D=0.1, ε_D=1.0 and ε_D=3 (dotted, dot-and-dash and dashed lines, respectively).

One may notice a significant difference between the two profiles as calculated by the proposed and the HLL model for large dimensionless dispersion (ε_D=1.0 and 3.0); the difference is negligible for ε_D less than 0.1. The dependence of the particle flux at X=1 on the dimensionless dispersion ε_D is plotted in Fig. 7 for the proposed model (solid line) and the HLL model (dashed line). As mentioned before, the particle flux predicted by the proposed model is independent of dispersion for the steady-state regime (Eq. (C-6)), which implies that the solid line is horizontal.

Consider the asymptotic case where the Peclet number vanishes. As $\varepsilon_D \gg 1$, the flux in the HLL model tends to unity; hence the steady-state flux is constant along the column and no particle is captured, which is unphysical. For large dispersion, the advective flux is relatively low; the capture rate in the HLL model is proportional to the advective flux and, therefore, is also

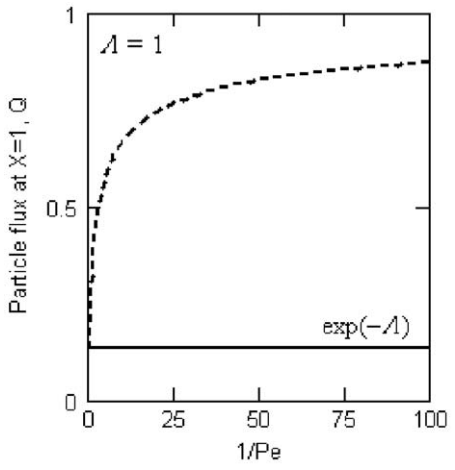

Fig. 7. Effect of dispersion on the flux at X= 1 for the steady-state mode in a semi-infinite reservoir for proposed and HLL models.

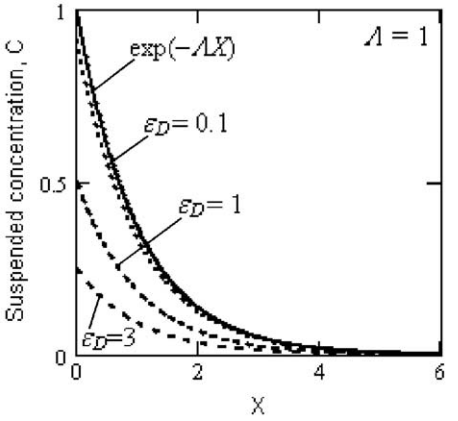

Fig. 8. Comparison between steady-state concentration profiles for deep bed filtration in a semi-infinite reservoir taking into account and neglecting dispersion in the inlet boundary conditions.

low. Thus, particle capture vanishes as $\varepsilon_D \gg 1$. No particle retention occurs when the dispersive mass transfer dominates over the advection.

The obtained contradiction occurs because the HLL model does not account for capture of particles transported by dispersive flux (Fig. 8).

6. Filtration in semi-infinite reservoir with simplified inlet boundary conditions

Let us discuss the case where dispersion is neglected in the inlet boundary condition (Eq. (14)). The exact solution is obtained in Appendix D, (Eq. (D-1)).

The concentration profile in steady-state regime (Eq. (D-2)) coincides with the concentration profile for the dispersion-free model. The simplified inlet boundary condition (Eq. (14)) is the same as the one for the dispersion-free model. Hence, the introduction of dispersion into the deep bed filtration model while keeping the same boundary condition (Eq. (14)) does not change the asymptotic profile of the suspended concentration.

Fig. 6 shows steady-state concentration profiles for the simplified inlet boundary condition, given by Eq. (D-2) (solid line) and for the complete inlet boundary condition, given by Eq. (C-5) (dotted curves). Three dotted curves correspond to ε_D=0.1, 1.0 and 3.0. The inlet concentration for dotted lines is always less than unity. The higher is the dispersion the lower is the stationary concentration under the fixed inlet flux.

7. Steady-state solution for filtration in finite cores

The expression for the particle flux profile in steady-state regime (Eq. (E-2)) coincides with the flux profile behind the mixture zone in semi-infinite media. The

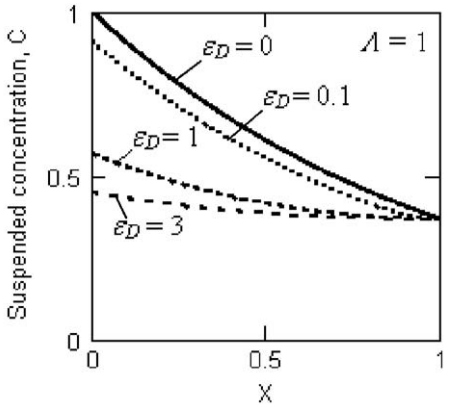

Fig. 9. Steady-state suspended concentration profiles for filtration in a limited core for $\varepsilon_D = 0$, 0.1, 1.0 and 3.0 (solid, dotted, dashed and dot-and-dash lines, respectively).

concentration profiles are different because the boundary condition of the dispersion absence is set at the core outlet $X = 1$ for the finite cores and at $X \to \infty$ for semi-infinite media.

The inlet concentration (Eq. (E-4)) is less than unity. It decreases as dispersion increases. By letting $\varepsilon_D \to \infty$ in Eq. (E-4), we find that the inlet concentration tends to $\exp(-\Lambda)$, which is the outlet concentration (Eq. (E-5)). Hence, as dispersion tends to infinity, the suspended concentration profile becomes uniform.

Fig. 9 shows suspended concentration profiles for $\varepsilon_D = 0.1$, 1.0 and 3.0. The inlet concentration for $\varepsilon_D = 0.1$ is equal to 0.91. For $\varepsilon_D = 3.0$ the profile is almost uniform.

It is important to emphasize that the outlet concentration (Eq. (E-5)) is independent of the dispersion coefficient and is determined by the filtration coefficient only. This fact is in agreement with the presented above interpretation of the filtration coefficient: λl is the probability for a particle to be captured by the sieve. The outlet concentration coincides with the particle flux due to the outlet boundary condition (Eq. (A-7)). Therefore, the outlet concentration under the steady-state conditions must be determined by the probability for a particle to be captured and must be independent of dispersion.

The outlet concentration predicted by the HLL model depends on the dispersion coefficient.

It is worth mentioning that the retention profile (Eq. (E-6)) is dispersion independent. This is because the capture rate is proportional to the total particle flux (Eq. (E-2)).

8. Treatment of laboratory data

The formula for steady state limit of the outlet concentration (Eq. (E-5)) allows determining the filtration coefficient from the asymptotic value of the breakthrough curve. From Eq. (E-5) it follows that

$$\Lambda = -\ln C(1) \tag{28}$$

Formula Eq. (28) coincides with that for determining the filtration coefficient from the asymptotic value of the breakthrough curve using the dispersion-free model (Eq. (26)), see (Pang and Sharma, 1994). The dispersion acts only in the concentration front neighbourhood, the asymptotic value for the breakthrough concentration is dispersion-independent.

Let us find out which model provides better fit to the experimental data. First, we determine the intervals for the test parameters where the difference between the modelling data by the two models is significant.

The proposed and HLL models differ by the delay term $\Lambda\varepsilon_D$ in the advective velocity. The models coincide as $\varepsilon_D = 0$. Hence, the larger is the dispersivity, the higher should be the difference between the two models.

Fig. 10 shows the core outlet flux for the steady-state regime with different Λ and ε_D as calculated by the proposed model (solid line) and the HLL model (dashed line). The marked points on dashed curves correspond to the value of ε_D where the difference between the proposed and HLL models starts to exceed 10%. For $\Lambda = 4$, 1 and 0.55, the 10%, the difference between the outlet fluxes can be observed for ε_D greater than 0.006, 0.13 and 1.74, respectively. The value $\Lambda = 4$ is typical for seawater injected in medium permeability cores. The value $\Lambda = 0.55$ is typical for virus transport in highly permeable porous columns. The typical core size $L = 0.1$ m. So, in order to validate the proposed and HLL models, one should perform laboratory coreflood with seawater in cores with dispersivity exceeding

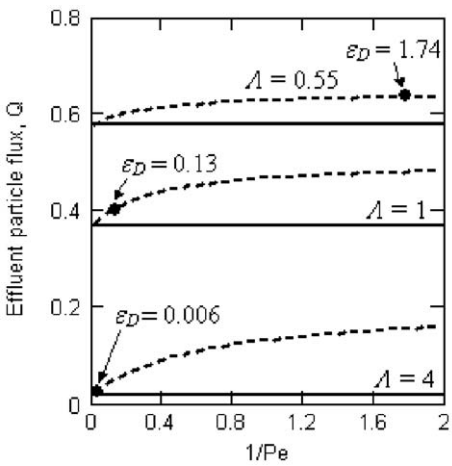

Fig. 10. Effect of dispersion on the particle flux at the core outlet for steady-state flows.

10^{-3} m; the core dispersivity for virus transport should exceed 0.2 m.

In papers by Ginn, 2002 and Jin et al., 1997, the outlet concentrations during the injection of particulate suspensions into sand porous columns were measured in laboratory tests. Flow experiments on the transport of oocysts bacteria and pathogenic viruses were carried out in these studies. Laboratory test parameters are presented in Table 1, where the first and the second lines correspond to tests presented in Ginn, 2002, four other tests are taken from the paper by Jin et al., 1997. The breakthrough curves in Fig. 11a, b correspond to tests 2 and 3. The filtration coefficients are calculated from the asymptotic values $C(X=1,\ T\rightarrow\infty)$ by Eq. (28) and are presented in Table 2.

In the laboratory tests in both works, the injected water was traced, and the tracer outlet concentrations were measured. Chloride and bromide tracers were used in order to determine the dispersion coefficient. The particle dispersion was assumed to be equal to the tracer dispersion. The values of dispersion coefficient are given in Table 1. Comparing the ε_D values in Fig. 10 and those in Table 1, one could conclude that there should be no significant difference between the proposed and HLL models for low values of dispersion in the laboratory tests.

Matching the laboratory data in limited cores by the analytical model for flow in a semi-infinite reservoir was suggested by Unice and Logan (2000). Fig. 11a and b depict breakthrough curves calculated by the analytical model (Eq. (C-2)) using the values of Λ and ε_D from Tables 1 and 2.

From Fig. 11a and b it is apparent that both models describe the experimental data equally well.

The difference between the filtration coefficients as predicted by the different models (second and third columns of the table) is not very high due to low dispersion of the porous media used in laboratory tests. A typical value of the filtration coefficient in Table 2 is $\Lambda=1.4$, and hence the two models would give different results for ε_D greater higher 0.15. The Table 1 shows that typical values of ε_D for tests 3–6 are 0.02, and hence a noticeable difference between the two models cannot be anticipated.

Table 1
Summary of experiments by Ginn (2002) and Jin et al. (1997)

Test no	Column length L (cm)	Flow rate J_w (cm/h)	Dispersion coeff. D (cm^2/h)	Dispersivity α_D (cm)	Dimensionless dispersion ε_D
Exp.1	10.0	29.6	7.70	0.26	0.026
Exp.2	10.0	2.96	0.53	0.18	0.018
Exp.3	20.0	3.35	1.23	0.37	0.02
Exp.4	20.0	3.19	1.13	0.35	0.02
Exp.5	20.0	3.11	1.13	0.36	0.02
Exp.6	10.5	2.99	0.76	0.25	0.02

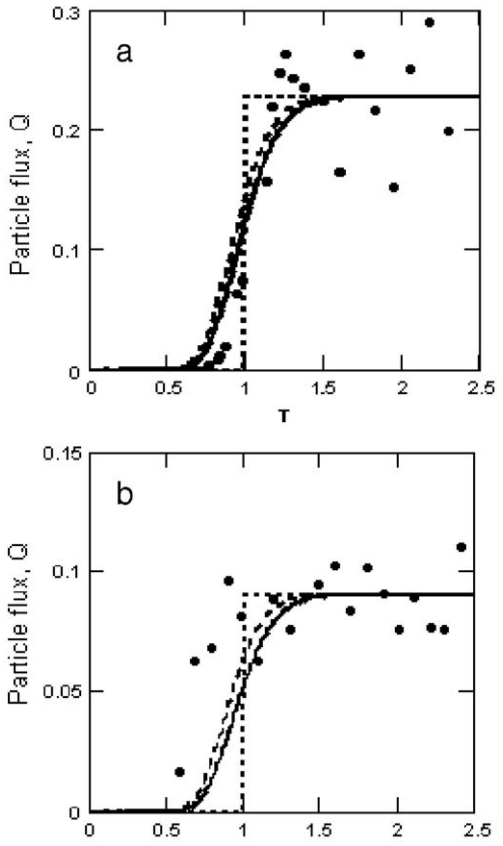

Fig. 11. Matching the breakthrough curves by the proposed and the HLL models (solid and dashed lines, respectively).

The proposed model assumes that the capture rate is proportional to the total flux, while the HLL model assumes that the capture rate is proportional to the advective flux only. Consequently, the flux in the capture kinetics of the HLL model is lower than that of the presented model. Therefore, the filtration coefficient should be higher in the HLL model rather than in the proposed model in order to fit the same retaining kinetics value.

The comparison between the second and the third columns of Table 1 shows that the filtration coefficient predicted by the HLL model is higher than that predicted by the proposed model which confirms the above presented speculations.

However, due to low dispersion in laboratory tests, the difference in the values of the filtration coefficient values from the two models is not sufficiently high for validation of the proposed and HLL models.

Table 2
Filtration coefficient as obtained from breakthrough curves by the proposed and the HLL models

Test no	Λ by proposed modeland by dispersion free model	Λ by HLL model
Exp.1	0.59	0.6
Exp.2	2.40	2.51
Exp.3	1.48	1.52
Exp.4	1.56	1.60
Exp.5	1.38	1.42
12/exp.6	0.75	0.76

The proposed and dispersion-free models give the same filtration coefficient value, because they use the same equation for the inverse problem (Eq. (28)).

For large ε_D, the values of Λ calculated by the two models would differ significantly. For example, for $\varepsilon_D=1$ and asymptotic outlet concentration $C=0.06$, the filtration coefficients predicted by the proposed and the HLL models are 2.8 and 7.1, respectively. The data from natural reservoir cores rather than that from sand columns may be used for validation of the model.

9. Travelling dispersion wave

Let us find the travelling wave solution for system (Eq. (20)) with dynamic blocking filtration coefficient (Eq. (5)):

$$C = C(w), S = S(w), w = X - uT \tag{29}$$

where u is the unknown wave speed.

The travelling wave solution of the deep bed filtration system (Eq. (20)) is described by non-linear dynamic system (Eq. (F-7)) in plane (C, S). The phase portrait is shown in Fig. 12. The analysis of the dynamic system is analogous to that performed by D. Logan (2001), for HLL model.

The system has two singular points. The point (0, 0) correspond to the initial conditions (Eq. (12)), i.e. to the absence of particles before the injection, and point (1, S_m), corresponds to the boundary condition (Eq. (14)), i.e. to the final equilibrium state (1,S_m), where S_m is the maximum number of retained particles per unit of rock volume. Point (0, 0) is a saddle point, the two orbits leaving the origin are unstable manifolds, and the two orbits entering the origin are stable manifolds. Point (1, S_m) is an unstable repulsive node.

As shown in Fig. 12, there is only one trajectory that links the two singular points, and this trajectory is the travelling wave solution. The travelling wave joins initial and final equilibrium states of a system.

The travelling wave speed (Eq. (F-6)) was calculated in Appendix F:

$$0<u=\frac{1}{1+S_m}<1 \tag{30}$$

At large length scale exceeding the travelling wave thickness, the wave (Eq. (29)) degenerates into shock wave. The speed (Eq. (30)) fulfils the Hugoniot condition of mass balance on the shock that corresponds to conservation law (Eq. (1)) (Bedrikovetsky, 1993). Therefore, the speed (Eq. (30)) for the proposed system (Eq. (20)) is the same as that for HLL model (Logan, 2001), since conservation law (Eq. (1)) is the same for either model.

The solution of initial-boundary value problem (Eqs. (12) and (14)) asymptotically tends to travelling wave for the case of blocking filtration function, (Eq. (5)). The travelling wave solution is invariant with respect to a shift along the axes x. The shift can be fixed at any time in order to provide an approximate solution for the initial-boundary value problem (Tikhonov and Samars-

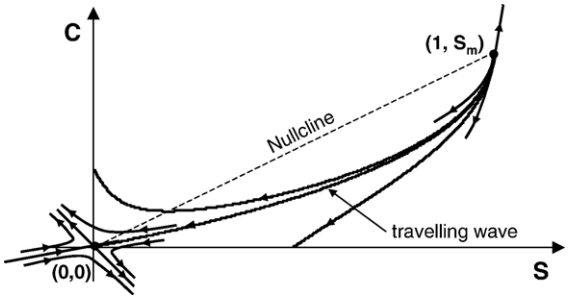

Fig. 12. Phase portrait of the dynamic system for dynamic blocking function.

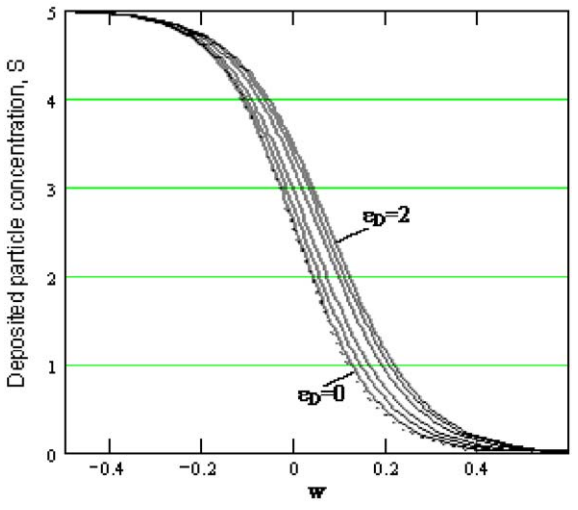

Fig. 13. Travelling wave solution without dispersion (traced line) and with dispersion (solid lines), for $_D$=0.03, 0.1, 0.2, 0.5, 1 and 2.

kii, 1990). Calculations in Appendix F show that the travelling wave fulfils the total mass balance for suspended and retained particles (Eq. (1)) if and only if it obeys the Goursat condition at the inlet $x=0$. It allows choosing the shift at any time T that the total mass balance is fulfilled, see Eqs. (F-14) and (15).

The retained concentration profiles are shown in Fig. 13 for several dispersion coefficients. The following data were used: linear blocking function (Eq. (6)) $\Lambda(S)=10-2S$, $c_0=100$ ppm and $\phi=0.2$. The dispersive wave ($\varepsilon_D>0$) travels ahead of the dispersion-free wave, and the wave velocities are equal. The higher is the dispersion coefficient the more advanced is the travelling wave.

10. Three dimensional deep bed filtration with dispersion

Let us derive three dimensional deep bed filtration of multi component suspension in porous media with size exclusion mechanism of particle capture on the macro scale. Particle populations with densities ρ_i, $i=1,2..n$, flow in porous rock with velocities U_i.

Particle capture in one dimension is modelled in Section 2 by a sieve sequence. The filtration coefficient λ_i for each population is defined as a fraction of particles captured per unit of the particle trajectory. We introduce the reference distance l between the sieve surfaces. Generally speaking, l is a continuous function of (x, y, z), where (x, y, z) is a point of three dimensional flow domain. A sieve captures $\lambda_i l$-th fraction of passing particles of i-th population, i.e. if $\rho_i U_i$ is a flux of i-th population particles entering the "core" which is perpendicular to the sieves, the particle capture rate is $\lambda_i l \rho_i U_i$, (Fig. 1).

The sieve surface has locally a plane form, so the sieves filling the three dimensional domain form two-dimensional vector bundle. Existence of a reference distance l between the sieve surfaces is consistent with the assumption of integrability of the vector bundle. Therefore, we consider the foliation case where the sieves are located on the surfaces where a smooth function $f(x,y,z)$ is constant.

For i-th population flux, the particle capture rate in a reference volume V is proportional to the flux projection on the vector perpendicular to the sieve. So, one-dimensional product $\lambda_i l \rho_i U_i$ (Eq. (4)) is substituted by the scalar product of the flux vector and the unit length vector perpendicular to the sieve:

$$\lambda_i \left\langle \frac{\nabla f}{|\nabla f|}, \rho_i U_i \right\rangle V \tag{31}$$

Therefore, the particle mass balance for i-th population with the consumption rate (Eq. (31)) becomes:

$$\frac{\partial \rho_i}{\partial t} + div(\rho_i U_i) = -\lambda_i \left\langle \frac{\nabla f}{|\nabla \mathrm{f}|}, \rho_i U_i \right\rangle \tag{32}$$

Introduce average mass density and velocity of the overall multi component flux

$$\rho = \sum_i \rho_i, U = \sum_i \frac{\rho_i U_i}{\rho} \tag{33}$$

The diffusive flux of i-th component around the front moving with the average velocity U is defined as a difference between the i-th component flux moving with the i-th component velocity and that with the average velocity (Landau and Lifshitz, 1987; Nikolaevskij, 1990)

$$\rho_i U_i = c_i \rho U - D_i \rho \nabla c_i \tag{34}$$

Assuming incompressibility of the mixture

$$\rho = const,\ divU = 0 \tag{35}$$

and substituting Eqs. (34) and (35) into Eq. (32), we obtain the following form of the particle mass balance for i-th population accounting for particle dispersion and capture

$$\frac{\partial c_i}{\partial t} + \langle U, \nabla c_i \rangle = D_i \Delta c_i - \lambda_i \left\langle \frac{\nabla f}{|\nabla f|}, c_i U - D_i \nabla c_i \right\rangle \tag{36}$$

Opening brackets of the scalar product in right hand side of Eq. (36) and grouping terms in the left and right hand sides, we obtain

$$\frac{\partial c_i}{\partial t} + \left\langle U - \lambda_i D_i \frac{\nabla f}{|\nabla f|}, \nabla c_i \right\rangle = D_i \Delta c_i - \lambda_i \left\langle \frac{\nabla f}{|\nabla f|}, U \right\rangle c_i \tag{37}$$

Eq. (37) is a three dimensional generalization of Eq. (16). It allows describing the anisotropy capture effect where the filtration coefficient depends on the flow direction, while three dimensional generalization of HLL Eq. (18) can describe just a scalar (isotropic) particle capture.

The first term in the scalar product in the left hand side of Eq. (37) consists of the average flow velocity U and the velocity with module $\lambda_i D_i$ directed perpendicular to sieve surfaces. So, the collective effect of dis-

persion with capture results in slowing down the advective particle flux.

11. Summary and conclusions

The particle size exclusion capture rate in deep bed filtration is proportional to the total particle flux including both the advective and the dispersive flux components. Therefore, the dispersion term must be present not only in the particle balance equation but also in the capture kinetics equation.

The outlet concentration for steady-state flow in a limited core is completely determined by the particle capture probability; therefore, it is independent of the dispersion coefficient. The outlet concentration by the model proposed is independent of dispersion, while that by the traditional HLL model is dispersion dependent.

The steady state flux profile in semi-infinite and limited size porous media should be also dispersion-independent, as the proposed model shows. The HLL model exhibits dependency of steady state flux profile on dispersion.

It allows concluding that for steady state flows the proposed model exhibits physically coherent results, while the traditional model exhibits physically unrealistic behaviour.

The collective effect of dispersion and capture on deep bed filtration in the model proposed is a delay in the propagation of the advective concentration wave.

A constant filtration coefficient can be determined from the asymptotical steady-state outlet concentration during a transient coreflood test using the proposed model without knowing the dispersion coefficient, while the dispersion coefficient should be known in order to calculate the filtration coefficient by the HLL model.

The constant filtration coefficient as determined from the asymptotical value of effluent concentration using the proposed model is equal to that determined by the dispersion-free model. Therefore, the HLL and the proposed models show equally satisfactory fit with the data of available experiments under small dispersivity.

Laboratory experiments in heterogeneous cores with high dispersivity should be carried out in order to validate the proposed model.

The travelling wave regime of deep bed filtration with dispersion exists for the blocking type of filtration coefficient only. The velocity of the travelling wave is determined by the maximum concentration of retained particles and is independent of dispersion coefficient. The higher is the maximum retained particle concentration the lower is the travelling wave speed.

The proposed three dimensional model allows describing anisotropic particle capture while 3D HLL model describes only scalar (isotropic) capture of suspended particles.

Nomenclature

c	Suspended particles concentration
c^0	Inlet suspended particles concentration
C	Dimensionless suspended particle concentration
D	Dispersion coefficient
k^0	Original permeability
l	Distance between sieves
p	Pressure
P	Dimensionless pressure
q	Particle flux
Q	Dimensionless particle flux
s	Laplace coordinate
S	Dimensioless retained particles concentration
t	Time
T	Dimensionless time
U	Darcy's velocity
v	Delay term in the advective velocity
x	Linear co-ordinate
X	Dimensionless co-ordinate
w	Transformation variable
α_D	Dispersivity
β	Formation damage coefficient
ε_D	Dimensionless dispersion coefficient
ϕ	porosity
λ	Filtration coefficient
Λ	Dimensionless filtration coefficient
μ	Suspension viscosity
σ	Retained particle concentration

Acknowledgements

The authors are grateful to Profs. Yannis Yortsos (South California University, USA), Oleg Dinariev (Institute of Earth Physics, Russian Academy of Sciences), Dan Marchesin (Institute of Pure and Applied Mathematics, Brazil) and Mikhael Panfilov (ENSG — INPL, Nancy, France) for the fruitful discussions. The collaboration with Adriano Santos (North Fluminense State University, UENF/Lenep, Brazil) is highly acknowledged.

Special thanks are due to Prof. Themis Carageorgos (UENF/Lenep) for support and encouragement.

Appendix A. Dimensionless governing equations

Introduction of dimensionless variables and parameters

$$X=\frac{x}{L},T=\frac{Ut}{\phi L},C=\frac{c}{c^0},S=\frac{\sigma}{c^0\phi},\Lambda(S)=\lambda(\sigma)L,$$
$$P=\frac{k_0p}{U\mu L},Q=\frac{q}{c^0U},\varepsilon_D=\frac{\alpha_D}{L} \tag{A-1}$$

transforms the governing Eqs. (1) (2) (4) and (9) to the following form:

$$\frac{\partial}{\partial T}(C+S)+\frac{\partial Q}{\partial X}=0 \tag{A-2}$$

$$\frac{\partial S}{\partial T}=\Lambda Q \tag{A-3}$$

$$Q=C-\varepsilon_D\frac{\partial C}{\partial X} \tag{A-4}$$

$$-\frac{1}{(1+\beta\phi c^0S)}\frac{\partial P}{\partial X}=1 \tag{A-5}$$

The boundary conditions (Eqs. (13) and (15)) in dimensionless variables (Eq. (A-1)) take the form:

$$X=0:Q=C-\varepsilon_D\frac{\partial C}{\partial X}=1 \tag{A-6}$$

$$X=1:\frac{\partial C}{\partial X}=0 \tag{A-7}$$

The simplified boundary condition (Eq. (14)) becomes:

$$X=0:C=1 \tag{A-8}$$

The initial conditions (Eq. (12)) remain the same.

Substituting the capture rate expression (Eq. (A-3)) into the mass balance Eq. (A-2), we obtain:

$$\frac{\partial C}{\partial T}+\frac{\partial Q}{\partial X}=-\Lambda Q \tag{A-9}$$

Substituting Eq. (A-4) into Eq. (A-9) yields the following parabolic equation:

$$\frac{\partial C}{\partial T}+v\frac{\partial C}{\partial X}=\varepsilon_D\frac{\partial^2C}{\partial X^2}-\Lambda C \tag{A-10}$$

$$v=1-\Lambda\varepsilon_D \tag{A-11}$$

Introduction of other dimensionless time, linear coordinate, pressure and filtration coefficient

$$X'=\lambda_0x,T'=\frac{U\lambda_0t}{\phi},\Lambda'(S)=\frac{\lambda(\sigma)}{\lambda_0},P'=\frac{k_0p\lambda_0}{U\mu} \tag{A-12}$$

keeps Eqs. (A-2) (A-3) and (A-5) the same; Eq. (A-4) becomes

$$Q=C-\varepsilon\frac{\partial C}{\partial X'},\varepsilon=\alpha_D\lambda_0 \tag{A-13}$$

Appendix B. Flow in an infinite reservoir

Let us consider flow in an infinite reservoir where, initially, water with particles was filling the semi-infinite reservoir $X<0$, and clean water was filling the semi-infinite reservoir $X>0$ (so-called Riemann problem):

$$T=0:C(X,0)=\begin{cases}1,X<0\\0,X>0\end{cases} \tag{B-1}$$

Boundary conditions $C=0$ and $C=1$ must be satisfied at $X\rightarrow\infty$ and $X\rightarrow-\infty$, respectively.

The filtration coefficient is supposed to be constant.

The solution for deep bed filtration in an infinite reservoir Eqs. (A-10) and (B-1) can be obtained in explicit form (Polyanin, 2002):

$$C(X,T)=\frac{1}{2}\left[\exp(-\Lambda T)erfc\left(\frac{X-vT}{2\sqrt{\varepsilon_DT}}\right)\right] \tag{B-2}$$

Appendix C. Transient solution for a semi-infinite reservoir

Let us discuss the particulate suspension injection into a semi-infinite reservoir, $X>0$. The initial and boundary conditions are defined by Eqs. (12) (A-6) (A-7), respectively. The condition $C=0$ for a semi-infinite reservoir should be satisfied at $X\rightarrow\infty$.

The explicit solution of the problem is obtained by substitution

$$C(X,T)=\exp(-\Lambda T)w(X,T) \tag{C-1}$$

and by Laplace transform in T (Polyanin, 2002):

$$\begin{aligned}C(X,T)=&\frac{1}{A}\exp\left[\frac{(v-A)X}{2\varepsilon_D}\right]erfc\left(\frac{X-AT}{B}\right)\\&-\frac{1}{A}\exp\left[\frac{(v+A)X}{2\varepsilon_D}\right]erfc\left(\frac{X+AT}{B}\right)\\&-\frac{(2-v)}{2\varepsilon_D}\exp\left(\frac{X}{\varepsilon_D}\right)\\&\times\int_0^T erfc\left(\frac{X+(2-v)t}{2\sqrt{\varepsilon_Dt}}\right)dt\end{aligned} \tag{C-2}$$

$$A=\sqrt{v^2+4\Lambda\varepsilon_D} \tag{C-3}$$

$$B=2\sqrt{\varepsilon_DT} \tag{C-4}$$

The solution (Eq. (C-2)) reaches steady state as $T \rightarrow \infty$:

$$C(X, \infty) = \frac{1}{1 + \Lambda\varepsilon_D} \exp(-\Lambda X) \tag{C-5}$$

Formula Eq. (C-5) is a steady-state solution of the boundary-value problem (x) and (x).

Eq. (C-5) allows calculation of the particle flux profile in the steady-state regime:

$$Q(X) = \exp(-\Lambda X) \tag{C-6}$$

Appendix D. Filtration in semi-infinite reservoir with simplified inlet boundary conditions

Let us discuss the simplified case where dispersion is neglected in the inlet boundary conditions. Eq. (A-10) is subject to initial condition Eq. (12) and to inlet boundary condition (Eq. (A-8)/Eq. (14)); the condition $C=0$ must be satisfied as $X \rightarrow \infty$.

The problem is solved using the Laplace transform in T (Polyanin, 2002):

$$C(X,T) = \frac{1}{2}\left[\exp\left(\frac{X}{\varepsilon_D}\right) erfc\left(\frac{X+MT}{B}\right) + \exp(-\Lambda X) erfc\left(\frac{X-MT}{B}\right)\right] \tag{D-1}$$

$$M = 1 + \Lambda\varepsilon_D$$

where constant B is given by formula Eq. (C-16).

The solution (Eq. (D-1)) tends to steady-state asymptotic as $T \rightarrow \infty$:

$$C(X, \infty) = \exp(-\Lambda X) \tag{D-2}$$

Appendix E. Steady-state solution for filtration in finite cores

The equation for steady state in finite cores corresponds to zero time derivative in Eq. (A-9):

$$\frac{dQ}{dX} = -\Lambda Q \tag{E-1}$$

The direct integration of the ordinary differential Eq. (E-1) taking into account the inlet boundary condition (Eq. (A-6)) results in the expression for the particle flux profile

$$Q = \exp(-\Lambda X) \tag{E-2}$$

which coincides with the flux profile (Eq. (C-16)) in semi-infinite media.

Substitution of the flux expression Eq. (E-2) into Eq. (A-4) leads to a first-order ordinary differential equation for suspended concentration profile. The solution that takes account of the outlet boundary condition Eq. (A-7) is given by

$$C(X) = \frac{1}{1 + \Lambda\varepsilon_D}\left[\exp(-\Lambda X) + \Lambda\varepsilon_D \exp\left(\frac{1}{\varepsilon_D}(X-1) - \Lambda\right)\right]. \tag{E-3}$$

The inlet concentration is calculated from Eq. (E-3):

$$C(0) = \frac{1}{1 + \Lambda\varepsilon_D}\left[1 + \Lambda\varepsilon_D \exp\left(-\frac{1}{\varepsilon_D} - \Lambda\right)\right] \tag{E-4}$$

The outlet concentration at $X=1$ is also obtained directly from Eq. (E-3):

$$C(1) = \exp(-\Lambda) \tag{E-5}$$

The outlet boundary condition (A-7) implies that the particle flux and the suspended concentration coincide at $X=1$.

The retention dynamics can be found from Eq. (A-3) using the expression for the particle flux (Eq. (E-2)):

$$S(X,T) = \Lambda T \exp(-\Lambda X) \tag{E-6}$$

Appendix F. Travelling wave solutions

Let us find travelling wave solutions

$$C = C(w),\ S = S(w),\ w = X - uT \tag{F-1}$$

for system Eq. (20), where u is an unknown wave speed.

The corresponding system of ordinary differential equations as obtained from Eq. (20) is

$$\frac{dS}{dw} = -\Lambda(S)(C+S) \tag{F-2}$$

$$\frac{dC}{dw} = \frac{1}{\varepsilon_D}[(1-u)C - uS] \tag{F-3}$$

The initial condition (12) for system Eq. (20) was already used during integration (Eqs. (21)–(24)), so the dynamic system (Eqs. (F-2) and (F-3)) fulfils the corresponding boundary condition:

$$w \rightarrow +\infty \ :\ C \rightarrow 0\ ;\ S \rightarrow 0 \tag{F-4}$$

The existence of the limited solution at minus infinity implies for Eq. (F-2) that $\Lambda(S_m)=0$, i.e. the filtration coefficient should be a blocking function, see Eq. (5). The corresponding boundary condition at minus infin-

ity for the dynamic system (Eqs. (F-2) and (F-3)) is obtained from the boundary condition (14):

$$w \to -\infty \ : \ C \to 1; \ S \to S_m \tag{F-5}$$

Substituting Eq. (F-5) with Eq. (F-3), we obtain the wave speed:

$$0 < u = \frac{1}{1+S_{\mathrm{m}}} < 1 \tag{F-6}$$

The wave speed (Eq. (F-6)) fulfils the Hugoniot condition of mass balance on the shock for conservation law (Eq. (1)).

The autonomous system (Eqs. (F-2) and (F-3)) can be reduced to one ordinary differential equation with unknown $C=C(S)$:

$$\frac{dC}{dS} = -\frac{(1-u)C - uS}{\varepsilon_D \Lambda(S)(C+S)} \tag{F-7}$$

A phase portrait of the dynamic system (Eq. (F-7)) is presented in Fig. 12. The analysis repeats that for the HLL system as performed by Logan, 2001. The system has a saddle singular point (0, 0) and an unstable repulsive node singular point (S_{m}, 0). There does exist the unique trajectory connecting two critical points that corresponds to the solution of the problem (Eqs. (F-2) and (F-3)).

The travelling wave solution is obtained by integrating Eq. (F-2):

$$w(S) = -\int^{S} \frac{1}{\Lambda(s)(C(s)+s)} ds + const. \tag{F-8}$$

The solution of the initial-boundary value problem (Eqs. (12) and (14)) tends asymptotically to the travelling wave (Eqs. (F-7) and (F-8)). It happens when T tends to infinity along each characteristic $X-uT=w=$const:

$$\lim_{T\to\infty} C(X,T)|_{w=const} = \lim_{T\to\infty} C(w+uT,T) = C(w) \tag{F-9}$$

$$\lim_{T\to\infty} S(X,T)|_{w=const} = \lim_{T\to\infty} S(w+uT,T) = S(w) \tag{F-10}$$

Following Tikhonov and Samarskii (1990), we approximate the solution of the problem (Eqs. (20) (12) and (14)) by the travelling wave for any finite T.

The initial-boundary problem (Eqs. (20) (12) and (14)) has the Goursat type and allows determination of the retained concentration at the inlet without finding the global solution. Fixing $C=1$ at $X=0$ in the retention kinetics (Eq. (A-3)) and dividing variables in the ordinary differential equation, we obtain

$$X = 0 : \ T = \int_0^{S(0,T)} \frac{dy}{\Lambda(y)} = \Phi(S) \tag{F-11}$$

The expression for retained concentration is obtained from Eq. (F-11) applying the inverse function

$$S(0,T) = \Phi^{-1}(T) \tag{F-12}$$

The travelling wave solution is invariant with respect to a shift $(X,T) \to (X+\mathrm{const}, T)$. Let us fix the constant w in Eq. (F-8) for each moment T in such a way, that the inlet retained concentration is the same as that in the solution of the initial-boundary value problem (Eq. (F-12)). So, Eq. (F-8) takes the form:

$$w(S,T) = -\int_{\Phi^{-1}(T)}^{S} \frac{1}{\Lambda(s)(C(s)+s)} ds - uT \tag{F-13}$$

Finally, the delay term in the travelling wave variable is chosen for any T in such a way, that the Goursat condition (Eq. (F-12)) is fulfilled.

Let us show that it provides with the total mass balance for the conservation law (Eq. (1)).

Substituting the travelling wave form (Eq. (F-1)) into the mass balance (Eq. (A-2))

$$\int_{-uT}^{\infty} (C+S) dw = T \tag{F-14}$$

and performing integration in x , from the Eq. (F-13) we obtain

$$T = \int_{-uT}^{\infty} (C+S) dw = \int_0^{S(-uT)} \frac{ds}{\Lambda(s)} = \Phi(S(-uT)) = \Phi(S(0,T)) \tag{F-15}$$

So, the solution (Eq. (F-13)) fulfils the integral mass balance for the domain $0<X<8$.

Solution in the plane (X, T) for the retained particle concentration can be obtained by substituting $w=X-uT$ into Eq. (F-13):

$$X(S,T) = -\int_{\Phi^{-1}(T)}^{S} \frac{1}{\Lambda(s)(C(s)+s)} ds \tag{F-16}$$

Eq. (F-16) is an approximate solution for initial-boundary value problem (Eqs. (12) and (14)).

References

Bedrikovetsky, P.G., 1993. Mathematical Theory of Oil and Gas Recovery. Kluwer Academic Publishers, Dordrecht.

Bedrikovetsky, P.G., Marchesin, D., Checaira, F., Serra, A.L., Resende, E., 2001. Characterization of deep bed filtration system from laboratory pressure drop measurements. J. Pet. Sci. Eng. 64, 167.

Bedrikovetsky, P., Marchesin, D., Hime, G., Alvarez, A., Marchesin, A.O., Siqueira, A.G., Souza, A.L.S., Shecaira, F.S., Rodrigues, J.R., 2002. "Porous media deposition damage from injection of water with particles," VIII Ecmor European Conference on Mathematics in Oil Recovery, Sept. 3–6, Austria, Leoben.

Bolster, C.H., et al., 1998. A method for calculating bacterial deposition coefficients using the fraction of bacteria recovered from laboratory columns. Environ. Sci. Technol. 32, 1329.

Danckwerts, P.V., 1953. Continuous flow systems: distribution of residence times. Chem. Eng. Sci. 2, 1.

Elimelech, M., et al., 1995. Particle Deposition and Aggregation: Measurement, Modelling, and Simulation. Butterworth-Heinemann, Oxford, England.

Ginn, T.R., 2002. A travel approach to exclusion on transport in porous media. Water Resour. Res. 38, 1129.

Grolimund, D., et al., 1998. Transport of in situ solubilized colloidal particles in packed soil columns. Environ. Sci. Technol. 32, 3562.

Harter, T., et al., 2000. Colloid transport and filtration of *Cryptosporidium parvum* in sandy soils and aquifer sediments. Environ. Sci. Technol. 34, 62.

Herzig, J.P., Leclerc, D.M., Goff, P.L., 1970, May. Flow of suspensions through porous media — application to deep filtration. Ind. Eng. Chem. 62 (5), 8.

Iwasaki, T., 1937. Some notes on sand filtration. J. Am. Water Works Assoc. 29, 1591.

Jensen, J.L., et al., 1997. J. Statistics for Petroleum Engineers and Geoscientists. Prentice Hall PTR, New Jersey.

Jin, Y., et al., 1997. Sorption of viruses during flow through saturated sand columns. Environ. Sci. Technol. 31, 548.

Kampen, Van N.G., 1984. Stochastic Processes in Physics and Chemistry. North-Holland, Amsterdan–Oxford.

Kechagia, P., Tsimpanogiannis, I., Yortsos, Y., et al., 2002. On the upscaling of reaction-transport processes in porous media with fast or finite kinetics. Chem. Eng. Sci. 57 (13), 2565.

Khilar, K.C., Fogler, H.S., 1998. Migration of Fines in Porous Media. Kluwer Academic Publishers, Dordrecht–Boston–London.

Kretzschmar, R., Barmettler, K., et al., 1997. Experimental determination of colloid deposition rates and collision efficiencies in natural porous media. Water Resour. Res. 33, 1129.

Kuhnen, F., Barmettler, K., et al., 2000. Transport of iron oxide colloids in packed quartz sand media. J. Colloid Interface Sci. 231.

Lake, L.W., 1989. Enhanced Oil Recovery. Prentice Hall, Englewood Cliffs.

Landau, L.D., Lifshitz, E.M., 1987. Fluid mechanics. (2nd ed.). Course of Theoretical Physics, vol. 6. Pergamon Press, Oxford.

Logan, D.J., 2001. Transport Modeling in Hydrogeochemical Systems. Springer.

Massei, N., et al., 2002. Transport of particulate material and dissolved tracer in a highly permeable porous medium: comparison of the transfer parameters. J. Contam. Hydrol. 57, 21.

Nikolaevskij, V.N., 1990. Mechanics of Porous and Fractured Media. World Scientific, New Jersey–Hong Kong.

Pang, S., Sharma, M.M., 1994. A model for predicting injectivity decline in water injection wells. SPE paper 28489 presented at 69th Annual Technical Conference and Exhibition held in New Orleans, LA, 25–28 September.

Payatakes, A.C., et al., 1974. Application of porous medium models to the study of deep bed filtration. Can. J. Chem. Eng. 52, 727.

Polyanin, A.D., 2002. Handbook on linear partial differential equations for scientists and engineers. Chapman and Hall CRC Press, Boca Raton–London.

Santos, A., Bedrikovetsky, P.G., 2005. Population balance model for deep bed filtration with pore size exclusion. J. Comput. Appl. Math 23 (2–3), 1–26.

Sharma, M.M., Yortsos, Y.C., 1987a. Transport of particulate suspensions in porous media: model formulation. AIChe J. 33 (10), 1636.

Sharma, M.M., Yortsos, Y.C., 1987b. A network model for deep bed filtration processes. AIChE J. 33 (10), 1644–1653.

Sharma, M.M., Yortsos, Y.C., 1987c. Fines migration in porous media. AIChE J. 33 (10), 1654–1662.

Sorbie, K., 1991. Polymer-improved Oil Recovery. CRC Press, Boca Raton–London.

Tiab, D., Donaldson, E.C., 1996. Petrophysics. Gulf Publishing, Houston.

Tikhonov, A.N., Samarskii, A.A., 1990. Equations of Mathematical Physics. Dover, New York.

Tufenkji, N., et al., 2003. Interpreting deposition patterns of microbial particles in laboratory-scale column experiments. Environ. Sci. Technol. 37, 616.

Unice, K.M., Logan, B.E., 2000. Insignificant role of hydrodynamic dispersion on bacterial transport. J. Environ. Eng. 126, 491.

van Genuchten, Th.W., 1981. Analytical solutions for chemical transport with simultaneous adsorption, zero-order production and first-order decay. J. Hydrol. 49, 213.

Wennberg, K.E., Sharma, M.M., 1997. Determination of the filtration coefficient and the transition time for water injection. Proceedings of the SPE European Formation Damage Conference, SPE 38181, The Hague, The Netherlands, June 2–3.